Spin-singlet dimerization in La_2RuO_5 investigated using magnetic susceptibility and specific heat measurements

S. Riegg,* A. Günther, H.-A. Krug von Nidda, and A. Loidl
Experimental Physics V, Center for Electronic Correlations and Magnetism, University of Augsburg, D-86159 Augsburg, Germany

M. V. Eremin
Kazan Federal University, 420008 Kazan, Russian Federation

A. Reller
Resource Strategy, University of Augsburg, D-86159 Augsburg, Germany

S. G. Ebbinghaus
Solid State Chemistry, Martin-Luther University Halle-Wittenberg, D-06099 Halle, Germany
(Received 23 March 2012; revised manuscript received 11 August 2012; published 18 September 2012)

The origin of spin-dimerization and concomitant spin-gap opening in the triclinic phase of poly- and single-crystalline La_2RuO_5 at unusually high temperatures was investigated using magnetic susceptibility and specific-heat measurements. From the low-temperature crystal structure the formation of antiferromagnetically coupled Ru^{4+} ($S = 1$) dimers within the quasi-two-dimensional magnetic system can be deduced, resulting in a nonmagnetic singlet state. It was found that the antiferromagnetic coupling within the dimers is much stronger than the interaction with neighboring dimers. La_2RuO_5 exhibits a step-like change in the magnetic susceptibility at 161 K, indicating a first-order transition of combined magnetic and structural character. The size of the spin-gap has been estimated from the thermally activated behavior in the low-temperature dimerized phase and was found to be significantly different in the polycrystalline sample when compared to the results obtained from the single crystals. The magnetic entropy obtained from specific-heat measurements amounts to roughly $0.5R\ln(3)$, reflecting solely the contribution of spin degrees of freedom to the entropy change during the phase transition.

DOI: 10.1103/PhysRevB.86.115125 PACS number(s): 75.30.Kz, 75.25.−j, 75.40.−s, 75.30.Cr

I. INTRODUCTION

One- or two-dimensional magnetic oxides providing low-temperature structural transitions with the formation of a nonmagnetic singlet ground state are well known and intensively studied for $S = 1/2$ compounds.[1–8] However, there are only few examples for $S = 1$ systems with a singlet ground state, because usually 3D long-range order sets in due to residual interchain or interplane interactions.[9–11] From the theoretical point of view, the ground state of an ideal uniform antiferromagnetic Heisenberg chain with half integer spins is gapless, while in the case of integer spins a nonzero excitation gap is formed.[12] Nevertheless, even in half-integer spin chains an energy gap can open if pairs of neighboring spins dimerize forming a nonmagnetic singlet ground state. Spin dimerization accompanied by structural modification is known as spin-Peierls transition[13] and is sometimes observed in 1D systems. In 2D systems, the magnetic ground state crucially depends on the anisotropy of the exchange with Ising spins exhibiting a long-range ordered state, while Heisenberg spins show no magnetic phase transition at finite temperatures. XY systems provide no conventional long-range spin order but are characterized by the formation of vortex-anti-vortex pairs as described by Kosterlitz, Thouless, and Berezinskii.[14] Further surprise comes from the fact that the transition from 1D to 2D is by no means smooth: The ground state of spin-ladder materials sensitively depends on the number of legs.[15]

Ruthenium-based oxides display an enormous variety of structures and electronic ground states, including the p-wave superconductor Sr_2RuO_4 or the field-tuned quantum critical magnet $Sr_3Ru_2O_7$.[16] This variety results from the large number of oxidation states ($+3$, $+4$, $+5$) available for ruthenium but also from the fact that the $4d$ electrons behave somewhat in between localized and itinerant and that orbital ordering effects can play a substantial role in establishing the ground-state configuration.[17] For example, the metallic $LaRuO_3$ contains Ru^{3+} ions,[18] whereas pentavalent Ru is reported for the magnetically frustrated hexagonal perovskites $(La,Sr)_{4-z}RuO_{7+\delta}$.[19] The unusual appearance of site-ordered Ru^{4+} and Ru^{5+} ions is found for $Ba_5Ru_3O_{12}$ with a nominal Ru oxidation state of $+4.67$.[20] On the other hand, a statistical distribution of tetra- and pentavalent Ru ions was reported for $La_{2-x}Sr_xCu_{1-y}Ru_yO_{4-\delta}$ resulting in average Ru valencies between $+4$ and $+5$ in this series.[21]

In this manuscript we explore the transition into a nonmagnetic ground state observed for the layered ruthenate La_2RuO_5.[22,23] In this compound, layers of zig-zag chains of corner sharing RuO_6 octahedra with Ru^{4+} ions carrying a spin $S = 1$ are separated by nonmagnetic LaO layers. At high temperatures, La_2RuO_5 behaves very close to a two-dimensional magnet but undergoes dimerization at 161 K, strongly coupled to structural distortions. At low temperatures, the ground state can be described best as a two-leg ladder with rungs forming spin-singlets. This transition seems to be a unique feature in two-dimensional integer spin arrangements and it seems worthwhile to investigate this dimerization-driven phase transition in more detail.

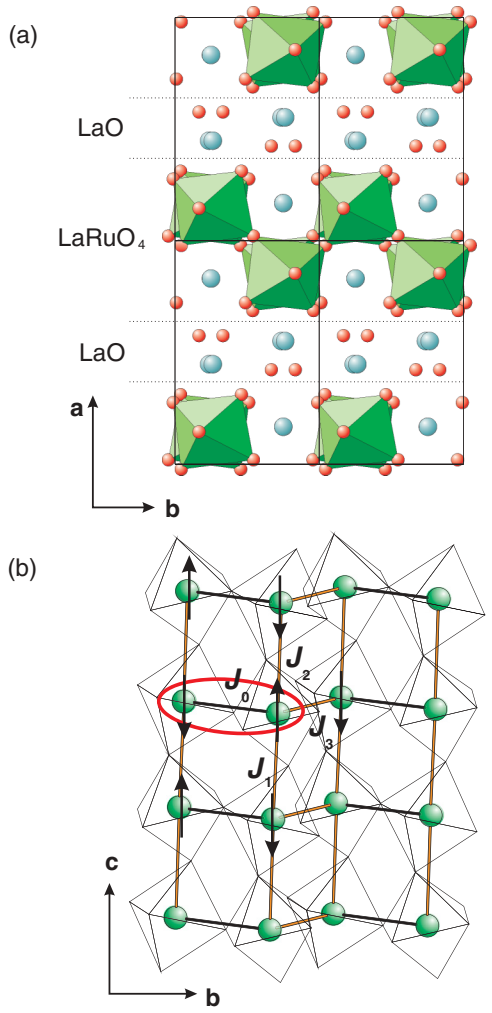

FIG. 1. (Color online) (a) Crystal structure of La_2RuO_5 (2×2 unit cells) viewed along the c axis. La is represented by turquoise spheres, oxygen by red spheres, and RuO_6 octahedra are drawn in light green. The alternating layering of LaO and $LaRuO_4$ along the a axis is indicated by dashed lines. (b) RuO_6 octahedra network (transparent) in the bc plane of the $LaRuO_4$ layers. One ruthenium (green spheres) dimer is marked by a red ellipse and the exchange paths are denoted J_0 to J_3. For details see text.

La_2RuO_5 exhibits a layered crystal structure [Fig. 1(a)] consisting of alternating perovskite-like $LaRuO_4$-layers and buckled LaO-layers along the crystallographic a axis.[22–24] At $T = 161$ K La_2RuO_5 shows a structural phase transition. The high-temperature (ht) phase crystallizes in the monoclinic space group $P2_1/c$ (No. 14), while the low-temperature (lt) phase exhibits triclinic symmetry ($P = 1$, No. 2). Both phases are semiconducting with small band gaps. For the ht-phase in polycrystals 0.15(5) eV has been found by electrical resistivity measurements, while for the lt-phase a slightly increased band gap of 0.21(5) eV was reported.[22,25]

The spin-gap formation in lt-La_2RuO_5 was first described as an orbital-ordering effect, which quenches the local Ru moments.[22] Later it was argued that it seems rather unlikely that the crystal-field splitting of the Ru t_{2g} levels exceeds Hund's rule coupling and it has been proposed that La_2RuO_5 is a further example of an orbitally induced Peierls state.[26] In fact, x-ray absorption spectroscopy[27] and muon-spin-rotation measurements[28] documented the existence of $S = 1$ spins in the lt-phase. The antiferromagnetic (AFM) exchange interaction between the Ru ions leading to the spin-Peierls-like ordering and singlet formation continues along the Ru-O-Ru paths in the $LaRuO_4$ layers. This interpretation was supported by density functional theory (DFT) calculations applying an augmented spherical wave (ASW) approach and a local density approximation (LDA), respectively.[27,29,30] The spin-Peierls scenario is corroborated by the fact that in the lt-phase alternating long and short Ru-O-Ru distances are found along the b axis. The Ru-Ru dimers form rungs of weakly interacting spin-ladders in the crystallographic c direction. The situation becomes more complicated due to the alternating distances between the rungs in the ladders, which require the introduction of an additional exchange parameter. The spin-ladder model was mainly derived from the exchange values J_i obtained from DFT calculations, including spin-polarized LDA and a Hubbard-U.[27] The corresponding Ru-Ru distances, Ru-O-Ru angles, and the exchange paths denoted as J_0 to J_3 for the ht- and lt-phase are listed in Table I and depicted in Fig. 1(b).

TABLE I. The Ru–Ru distances and Ru–O–Ru angles ϑ linked to the exchange couplings J_i as shown in Fig. 1 b.

J_i	d(Ru-Ru) (Å)	ϑ(Ru-O-Ru) (deg)
ht-phase		
J_0, J_3	3.975	155.4
J_1, J_2	3.978	152.8
lt-phase		
J_0	3.868	160.2
J_1	3.923	150.6
J_2	4.036	151.0
J_3	4.045	153.2

In the ht-phase a regular sublattice with almost identical Ru-Ru distances of roughly 3.975 Å is found while the Ru-O-Ru angles show values of approximately 155.4° in b direction and 152.8° along the c axis [Table I and Fig. 1(b)].[24] This arrangement indicates AFM exchange interactions with similar values for the corresponding exchange constants J_i. In contrast, in the lt modification the distances and angles are distinctly different (Table I). These structural changes lead to anisotropic variations of the J_i as deduced from DFT calculations and, therefore, strongly support the singlet model [Fig. 1(b)]. From the inspection of the Ru-Ru distances and the Ru-O-Ru bond angles ϑ as documented in Table I, it is plausible that at 161 K La_2RuO_5 transforms from an almost 2D Heisenberg paramagnet into a spin ladder with spin singlets along the rungs parallel to the c axis. This model is analyzed using magnetic susceptibility and heat-capacity measurements.

II. EXPERIMENTAL RESULTS AND DISCUSSION

A. Basic theoretical considerations

In accordance with the models reported in previous publications for the magneto-structural transition in La_2RuO_5 we start from the strong crystal-field approach for the ht-phase. The

octahedral crystal field splits the 4*d* electronic states of Ru in e_g and t_{2g} levels. The energetically lower-lying configuration in Ru^{4+} is t_{2g}^4, which is equivalent to t_{2g}^2 in hole representation. As it was pointed out in Refs. 22 and 27, the distorted octahedral crystal field stabilizes the state $\{d_{xz}^{\uparrow},d_{xz}^{\downarrow}\}$. The x and y axes are lying in the crystallographic ab plane but are rotated by 45° with respect to the crystallographic axes a and b, while z and c are aligned parallel. Coulomb-repulsion between the remaining fourfold degenerate states $\{d_{xy}^{\alpha},d_{yz}^{\beta}\}$ splits them into a singlet state

$$1/\sqrt{2}[\{d_{xy}^{\uparrow},d_{yz}^{\downarrow}\}-\{d_{xy}^{\downarrow},d_{yz}^{\uparrow}\}]$$

and a triplet

$$|M_S=1\rangle=\{d_{xy}^{\uparrow},d_{yz}^{\uparrow}\}$$
$$|M_S=-1\rangle=\{d_{xy}^{\downarrow},d_{yz}^{\downarrow}\}$$
$$|M_S=0\rangle=1/\sqrt{2}[\{d_{xy}^{\uparrow},d_{yz}^{\downarrow}\}+\{d_{xy}^{\downarrow},d_{yz}^{\uparrow}\}].$$

According to Hund's rules, the triplet state is energetically lower and can be described by the effective spin $S=1$. The orbital momentum is quenched. This configuration is already energetically favored by the octahedral deformations in the ht-phase and becomes further stabilized by the structural changes occurring during the transition to the lt-phase.

The superexchange interaction between cations with t_{2g}^n configuration via intermediate oxygens can be described according to[31,32]

$$J=J_{90}\sin^2\vartheta+J_{180}\cos^2\vartheta, \quad (1)$$

where ϑ is the Ru-O-Ru angle listed in Table I. J_{90} and J_{180} are the values of the superexchange coupling parameters at $\vartheta=90°$ and $\vartheta=180°$, respectively. On the basis of the Goodenough-Kanamori-Anderson rules, it is expected that $J_{180}>|J_{90}|$.[33] In addition, it should be noted that J_{180} strongly increases due to the shortening of the Ru-O distances during the magneto-structural transition, because its value is proportional to the Ru,O-transfer integral $t_{Ru,O}$ to the power of four: $J_{180}\sim[t_{(Ru,O)}^4/\Delta_{(Ru,O)}^2\,U]$, with $\Delta_{Ru,O}$ representing the charge transfer and the Mott-Hubbard gap U.[34] Using Eq. (1) and the angles ϑ one can see that the superexchange coupling parameter J_0 increases due to the structural changes caused by the phase transition from the ht to the lt modification, while the values J_1, J_2, and J_3 decrease simultaneously. This finding strongly supports the introduced model of the spin-ladder with rungs consisting of dimerized Ru spins, as indicated in Fig. 1(b). This model also implies a strong increase of J_0 by probably orders of magnitude in the lt-phase compared to the other exchange interactions in agreement with the rather high transition temperature of 161 K and the reported opening of a spin-gap, which is a measure of the intradimer exchange J_0.[22]

B. Magnetic susceptibility

Polycrystalline samples of La_2RuO_5 were obtained by a soft-chemistry reaction based on the thermal decomposition of citrate precursors as described in detail elsewhere.[35] The process of obtaining flux-grown single crystals with maximum size of roughly $50\times50\times20$ μm^3 is described in Ref. 36. The magnetic susceptibilities were measured on a SQUID magnetometer (Quantum Design MPMS5) in the temperature range $2\leqslant T\leqslant300$ K. Field cooled conditions with different magnetic fields were applied.

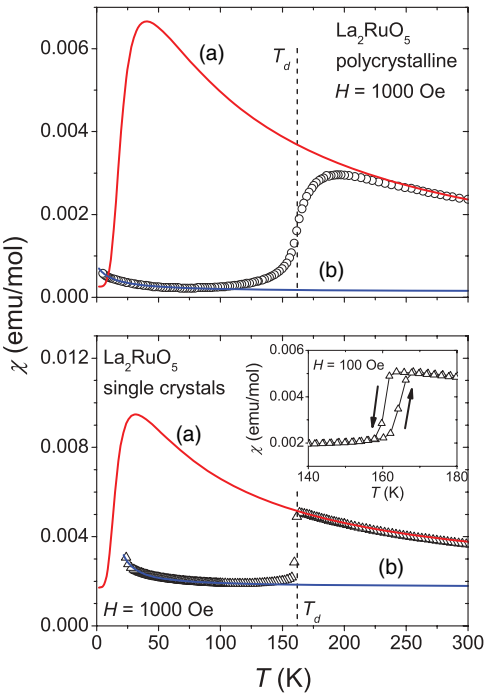

FIG. 2. (Color online) Top frame: Magnetic susceptibility of polycrystalline La_2RuO_5 from sol-gel reaction (open circles). Bottom frame: Susceptibility of flux grown La_2RuO_5 single crystals (open triangles). The solid red lines (a) mark the 2D Heisenberg model, and the solid blue lines (b) indicate the lt-Curie-Weiss fits of the low-temperature Curie tails. The inset in the lower frame shows the thermal hysteresis of the dimerization transition in the susceptibility of single crystalline La_2RuO_5.

In the upper frame of Fig. 2 the susceptibility $\chi=M/H$ at $H=1000$ Oe of La_2RuO_5 prepared from the sol-gel reaction is shown while in the lower frame χ of a batch of flux grown single crystals is depicted. The vertical dashed lines mark the dimerization temperature $T_d\approx161$ K of the Ru spin-moment pairing transition. Using conventional Curie-Weiss fits for $T\geqslant200$ K [$\chi=\chi_0+C_{ht}/(T-\Theta_{CW})$], effective magnetic moments $\mu_{eff}=2.89(2)\,\mu_B$ and $2.62(2)\,\mu_B$ for the poly- and single crystals were obtained, respectively. These values are in agreement with the Ru^{4+} spin-only value of 2.83 μ_B for $S=1$. The corresponding Curie-Weiss temperatures amount to $-177(12)$ K for the polycrystalline sample[35] and $-100(8)$ K for the single crystals, indicating AFM interactions. The value of χ_0 of the polycrystalline sample is 2.6×10^{-4} emu/mol, but considerably higher for the single crystals (1.72×10^{-3} emu/mol).

For a more sophisticated analysis, the 2D AFM Heisenberg model for a square planar lattice was compared to the measured susceptibilities.[37] The 2D AFM Heisenberg model was chosen due to the rather regular two-dimensional lattice of Ru^{4+} ions in the structurally isolated $LaRuO_4$ layers and the AFM interactions derived from Θ_{CW} occurring in the paramagnetic ht-phase. The calculated susceptibilities are marked by solid red lines (a) in Fig. 2 and were obtained

according to[37]

$$\chi = \chi_0 + \frac{N_A g^2 \mu_B^2 \mu_{eff}^2 S(S+1)}{3k_B T} \left(\sum_{n=0}^{6} a_n x^n \right)^{-1}. \quad (2)$$

The constants amount to $a_0 = 1$, $a_1 = -5.333$, $a_2 = 9.778$, $a_3 = -9.481$, $a_4 = 6.420$, $a_5 = -42.923$, $a_6 = 269.313$, and $x = -J_0/k_B T$. The values for a_n were calculated from equations given in Ref. 37, while J_0/k_B was fit using the temperature region above the transition step. The values of $J_0/k_B = 9$ K (sol-gel) and $J_0/k_B = 7$ K (single crystal) reveal AFM exchange interactions between the Ru ions. The 2D Heisenberg model probably would provide a reasonable description of the susceptibility, if no structural changes occurred. Nevertheless, the Heisenberg model is obviously not suitable to explain the susceptibility in the phase transition range and the magnetostructural phase transition is strongly enhanced when compared to the average magnetic exchange.

To estimate the concentration of paramagnetic centers, which do not take part in the dimerization, the small increases of χ below 50 K were also fit to a Curie-Weiss law and are marked by solid blue lines (b) in both panels of Fig. 2. The Curie constant of the polycrystalline sample amounts to $8.13(50) \times 10^{-3}$ emu K/mol, which corresponds to roughly 1% of the Curie constant of the ht-phase. This finding can be explained by a small number of nondimerized Ru spins due to the structural distortions, e.g., at grain boundaries. On the other hand, we cannot completely rule out the presence of an impurity phase, because its concentration would be close to the detection limit of x-ray powder diffraction. Θ_{CW} of the lt fit is negative [−12.6(8) K] and χ_0 is roughly reduced by a factor of two compared to the value calculated above (1.3×10^{-4} emu/mol). The absolute values are slightly smaller than reported by Khalifah *et al.* (Ref. 22) for a sample obtained by solid-state reaction. For the single crystals, a slightly increased value for the Curie constant [$16.38(60) \times 10^{-3}$ emu K/mol, roughly 2% of ht-phase Curie constant] was obtained and χ_0 amounts to 1.72×10^{-3} emu/mol, which is close to the value found for the Curie-Weiss fit in the high-temperature region. A small positive Curie-Weiss temperature [$\Theta_{CW} = 10.5(5)$ K] is found for the lt fit of the single crystalline sample.

To investigate the unexpected uprise found in the susceptibility of the single crystals at very low temperatures, additional magnetization hysteresis measurements have been performed for selected temperatures. The M versus H curves are depicted in Fig. 3. In the ht-phase a typical linear paramagnetic behavior is observed up to the highest available external field of 50 kOe. This paramagnetic behavior is also found in the lt-phase down to 50 K reflecting the absence of a ferromagnetic impurity in the sample. At 2 K, a broad and irregular shaped hysteresis is observed (Fig. 3), indicating the presence of a ferro- or ferrimagnetic phase with a small ordered moment of roughly 60 emu/mol as derived from the remanence. The shape at small fields is similar to the ones observed for layered thin antiferromagnetically ordered films (see, e.g., Refs. 38–40). The layered structure of La_2RuO_5 leads to twinned crystals, i.e., domains with alternating orientations.[36] By optical microscopy these domains can be observed as a fishbone shape contrast. The interaction between the crystal domains is comparable to the coupling between the thin films.

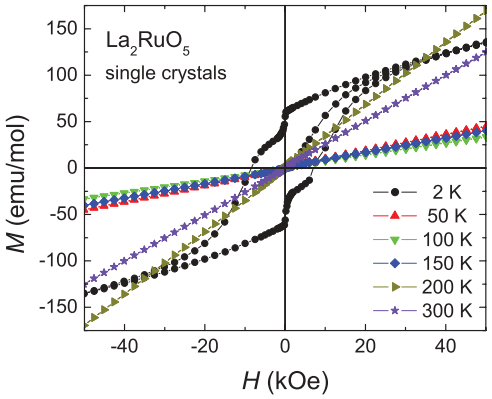

FIG. 3. (Color online) Magnetization hysteresis data of a batch of single crystalline La_2RuO_5 for selected temperatures.

Therefore, it can be assumed that the interaction of the domain layers causes hysteresis at low temperature as an intrinsic effect in the crystals. In polycrystalline samples the hysteresis is not observed because the size of the domains becomes too small for cooperative ordering.

The remarkable difference between the χ_0 values in the lt-phase of the two samples can be explained by a possible presence of $BaRuO_3$ in the single-crystal batch from the $BaCl_2$ flux. Since $BaRuO_3$ also forms black plate-like-shape crystallites, it cannot be distinguished visually. Due to a strong overlap of the peak positions, $BaRuO_3$ cannot be identified in the XRD pattern either. On the other hand, the increased intensity of a diffraction peak at $2\Theta = 31^\circ$ points to the presence of 4H-BaRuO3.[41] The metallic 4H-$BaRuO_3$ shows Pauli paramagnetism of approximately 1×10^{-3} emu/mol, which enhances the temperature-independent susceptibility of the single-crystalline La_2RuO_5 sample.[42]

To determine the spin-gap from the magnetic susceptibilities in the dimerized phase, the low-temperature Curie-Weiss fits including a constant χ_0 have been subtracted from the experimental results (χ_{korr}). As the temperature-independent susceptibility was significantly enhanced for the batch of the single crystals when compared to the results obtained for the polycrystalline sample, the former results bear a larger experimental uncertainty. From the residual magnetic susceptibilities of the lt-phase, the derivatives $d\chi_{korr}/dT$ have been calculated. The results are depicted in Fig. 4. Both data sets show symmetric peaks with a maximum close to the dimerization transition. Astonishingly, the observed peaks for both samples can well be fitted assuming Lorentzian profiles. The fits for both samples yield similar transition temperatures [$T_{d,sc} = 160.7(1)$ K and $T_{d,pc} = 161.9(2)$ K], but significantly different widths. The full width at half maximum (FWHM) is almost an order of magnitude larger for the polycrystalline sample than for the batch of single crystals ($FWHM_{sc} = 1.9(3)$ K, $FWHM_{pc} = 11.8(6)$ K). A word has to be said concerning the Lorentzian profile. If a mere static distribution of different crystal regions characterized by slightly varying ordering temperatures would be present, a Gaussian profile is expected. The Lorentzian line shape indicates a dynamic effect driven by a thermal broadening of a distribution of two-level systems characterized by singlet-triplet excitations. From the FWHM values it can be concluded that the thermal distribution

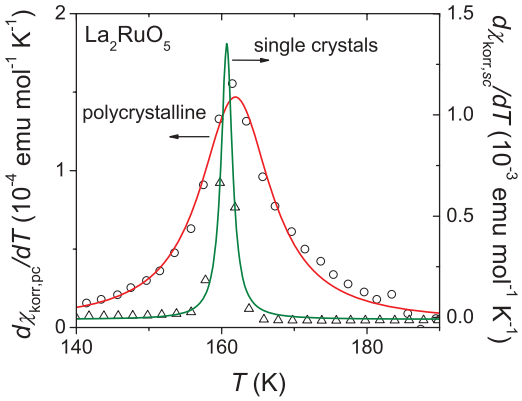

FIG. 4. (Color online) Derivatives of the magnetic susceptibilities for poly- (open circles) and single-crystalline (open triangles) La_2RuO_5. The susceptibilities have been corrected for the low-temperature Curie-Weiss contributions as indicated in Fig. 2. The solid lines correspond to Lorentzian-fits, centered at the phase transition temperature.

of two-level systems is much broader in the polycrystalline sample.

To obtain a value for the spin-gap from the residual low-temperature susceptibilities, Fig. 5 shows the logarithm of the magnetic susceptibility versus the inverse temperature, i.e., an Arrhenius type plot. Indeed, from approximately 150 K down to 70 K in the polycrystals and down to roughly 100 K in the single crystals, both susceptibilities reveal a strictly linear behavior but indicate drastically different spin-gap energies. The deviations at low temperatures reflect errors due to corrections of the lt-Curie-Weiss fits and the temperature-independent susceptibilities. The spin-gaps as derived from the linear fits amount to $\Delta_{pc} = 48(1)$ meV for the polycrystals and $\Delta_{sc} = 112(1)$ meV for the single crystals. The result

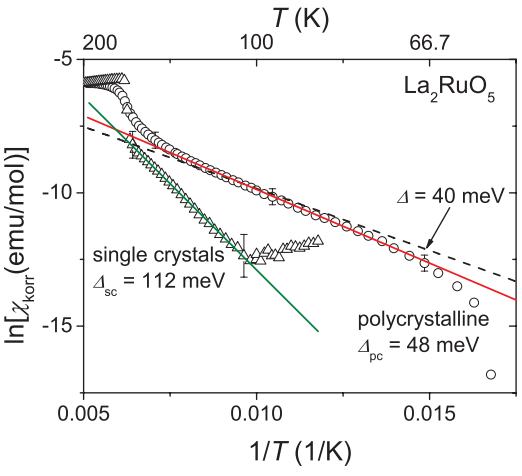

FIG. 5. (Color online) Arrhenius plots of the corrected susceptibilities in the low-temperature phase for poly- (open circles) and single-crystalline (open triangles) La_2RuO_5. The solid lines are linear fits assuming an Arrhenius behavior, resulting in spin-gaps of $\Delta_{pc} = 48$ meV and $\Delta_{sc} = 112$ meV for poly- and single-crsytalline samples, respectively. The Arrhenius behavior characteristic for a spin-gap of $\Delta = 40$ meV as observed by inelastic neutron scattering is indicated as dashed line.

for the polycrystalline sample comes close to the spin-gap value obtained by inelastic neutron scattering, which was of the order of 40 meV (Ref. 22), and the related Arrhenius behavior is indicated as dashed line in Fig. 5. However, the spin-gap for the single crystals is significantly larger. The fact that the results of poly- and single-crystalline samples differ significantly has also been observed in the determination of the charge gap (Ref. 22), where values of roughly 0.21 eV have been observed for single crystals, while a value of 0.32 eV for polycrystalline samples was found. Malik *et al.* (Ref. 25) reported a charge gap of even only 0.16 eV for the polycrystals. Thus, we conclude that the gaps in La_2RuO_5 are extremely sensitive to even small structural variations between samples. This can be already anticipated regarding the strong increase of the exchange constant J by two orders of magnitude at the dimerization transition, which is dominantly driven by the structural changes, reflecting only weakly modified bond angles and interatomic distances. Different preparation routes and internal strains in the twinned single crystals certainly provide slight variations of the structural parameters. It should also be noted that the inelastic peak in the neutron data (Ref. 22) extends up to 120 meV (including the single-crystal value of 112 meV), reflecting the broad distribution of gap values in polycrystalline material.

From a comparison of the measurements obtained for the poly- and single-crystalline sample it can be concluded that the dimerization transition is of first order. This is especially documented for the single-crystalline sample, while in the polycrystals this first-order transition is smeared out. The first-order character of the transition in the single crystals is supported by the thermal hysteresis of χ shown in the inset of Fig. 2, where a shift of roughly 4 K between the heating and the cooling curve was observed.

Neither changes of the phase-transition temperatures nor of the obtained J_0 values were detected upon varying the external magnetic field H between 100 Oe and 50 kOe. Such a shift was reported to be typical for $S = 1/2$ spin-Peierls transitions.[43] Thus, the transition in La_2RuO_5 is unconventional for $S = 1$ from both theoretical calculations (Ref. 44) and our experimental results similar to the 1D antiferromagnetically ordered chains with $S = 1/2$ and $S = 1$ described by Haldane.[12]

C. Specific heat

The specific heat at constant pressure C_p was measured between 1.8 and 300 K using a PPMS by Quantum Design. In the range of the observed peak (±15 K) as well as below 30 K, the specific heat was recorded in steps of 0.2 K, while steps of 1 K were applied for all other temperatures. Approximately 10 mg of the polycrystalline sample powder and 2 mg of polyvinyl alcohol (PVA) were mixed, ground in an agate mortar, and pressed into a pellet of 3-mm diameter. The contribution of the PVA was subtracted from the data. The fit of the lattice contribution was performed with the program Mathematica 7 applying an Einstein-Debye 3D phonon model, omitting the peak range between 140 and 180 K as deduced from the susceptibility data.

The specific heat in C_p/T representation is depicted in the top frame of Fig. 6. Also shown is the Einstein-Debye fit, which was performed according to Ref. 45 to model the

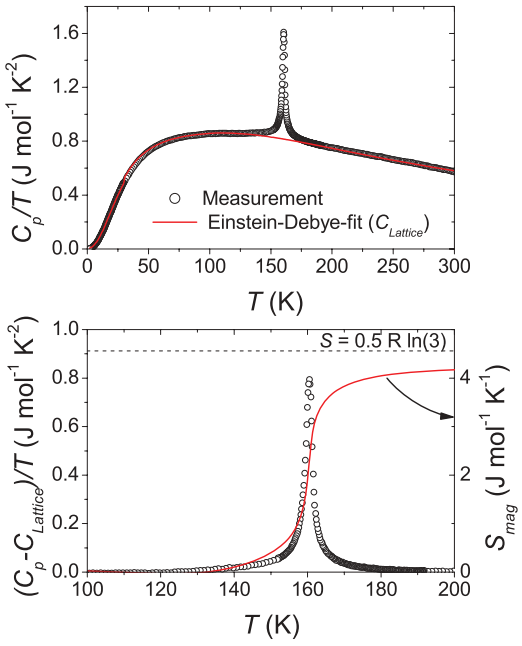

FIG. 6. (Color online) Top frame: C_p/T of polycrystalline La_2RuO_5 (symbols) and Einstein-Debye fit (solid red line). Bottom frame: Data after subtraction of the Einstein-Debye fit ($(C_p - C_{\rm Lattice})/T$; symbols) and $S_{\rm mag}$ obtained from integration of the residual curve (solid red line).

lattice contribution to C_p. For the fit one temperature term was used for each atom per formula unit, i.e., $1 \times \Theta_{\rm D}$ ($\Theta_{\rm D}$: Debye-temperature) and $7 \times \Theta_{\rm E}$ ($\Theta_{\rm E}$: Einstein-temperature). To reduce the number of parameters, four of the Einstein terms were set equal, reflecting the oxygen octahedra in the $LaRuO_4$ layers. According to the semiconducting behavior of La_2RuO_5, a very small Sommerfeld coefficient of roughly 2.2 mJ mol^{-1} K^{-2} was used in agreement with previously reported results to increase the fit quality.[25] The following values for the five fitting parameters corresponding to the number of independent lattice sites were obtained: $\Theta_{\rm D} = 132(1)$ K, $\Theta_{\rm E1} = 175(1)$ K, $\Theta_{\rm E2} = 217(2)$ K, $\Theta_{\rm E3} = 325(3)$ K, and $(4\times)\Theta_{\rm E4} = 520(3)$ K.

To determine the specific heat of the phase transition, the Einstein-Debye fit was subtracted from the experimental data. The residual $(C_p - C_{\rm Lattice})/T$ depicted in the bottom frame of Fig. 6 shows a sharp peak, indicating a first-order transition. This transition can be attributed to the abrupt change of exchange interaction due to the structural transition, which is clearly observable in the bottom frame of Fig. 2. To obtain the excess entropy, $(C_p - C_{\rm Lattice})/T$ was integrated between 75 and 250 K according to $S_{\rm exc} = \int C_p/T dT$. The integral is depicted in the bottom frame of Fig. 6 (solid red line). A value of $S_{\rm exc} = 4.2(3)$ J mol^{-1} K^{-1} was obtained.

For the ordering of a simple $S = 1$ antiferromagnetic spin system, a theoretical value of $S_{\rm mag} = R\ln(2S+1) \approx 9.13$ J mol^{-1} K^{-1} is expected (R: gas-constant). A value of approximately 8.3 J mol^{-1} K^{-1} was described in literature for La_2RuO_5 but a rather simple approach was used to model the lattice contribution.[25] The Einstein-Debye fit applied in this work is a more reliable description of the phonon contributions. The distinctly smaller excess entropy obtained from our data can be explained taking into account the lt-phase spin-singlets. The molar entropy is defined $S_{\rm mag} = k_{\rm B}\ln(\Omega)$, where Ω is the partition function. As already stated in Sec. II A, the quenched orbital momentum does not change at the phase transition. Therefore, the orbital degrees of freedom do not contribute to the entropy change. Reasoned by this, we only take into account the spin degrees of freedom. In a simple model, the entropy change at T_d from the paramagnetic ht-phase to the the dimerized lt-phase is given by $\Delta S = |R\ln 3 - 0.5 S_{\rm dimer}|$. The latter term describes the entropy of the dimerized state $S_{\rm dimer} = \bar{E}/T + k_{\rm B}\ln Z$, which has to be multiplied by 0.5 to compensate the reduced number of dimers compared to the number of single spins in the ht-phase. Z denotes the partition function of the energy spectrum of the dimers with a singlet ground state, a triplet as first excited state, and a quintuplet as second excited state. $\bar{E}$ is the thermally averaged energy of the three states. Using the thermal distribution function, the entropy change at T_d can be calculated depending on $J_0/(k_{\rm B}T_d)$. In turn, the intradimer exchange J_0 can also be determined from the obtained experimental entropy, which is in first approximation $0.5R\ln 3$ (Fig. 6), reflecting a significant contribution of the dimer state to the entropy change. The value of $J_0/k_{\rm B} \approx 260$ K (23.5 meV) is obtained as lower estimate of the lt-phase intradimer exchange from the experimental entropy. The value for J_0 is smaller than the spin-gaps determined by magnetization measurements; however, in this simple entropy model the interdimer interaction is neglected and the correlation between the gap and J_0 has to be further investigated. It should be recalled that the structural degrees of freedom may also contribute to the observed excess entropy; however, this contribution seemingly is very small.

III. SUMMARY AND CONCLUSION

La_2RuO_5 is a rare example of a transition-metal oxide forming a 2D spin lattice with a spin-dimerization transition. It is argued that this transition might be triggered by the orbital degrees of freedom. Indeed, Hotta and Dagotto[46] pointed out that ruthenates may undergo orbital ordering despite their quite extended $4d$ orbitals. From a formal point of view Ru^{4+} in the low-spin configuration has two holes in the t_{2g} triplet and is Jahn-Teller active. However, in canonical Jahn-Teller systems the local structural units (i.e., octahedra) that surround the Jahn-Teller active ions are strongly deformed. This is only, to a limited degree, the case in the ht modification of La_2RuO_5, where the bonds connecting the octahedra are only slightly changed.[24] It is rather the buckling and twisting of the octahedra creating shortened and elongated Ru-O-Ru distances. In perovskites, this is known to result from structural constraints due to different ionic radii of the components. As derived from the energy level scheme, orbital order is realized above T_d and, therefore, the dimerization transition in La_2RuO_5 is basically driven by the structural changes stabilizing the orbital ground state.

The concomitant structural phase transition results in only slightly changed Ru-O-Ru distances and bonding angles, which nonetheless significantly affects the spin-spin interaction strength of the Ru^{4+} ions. Similar exchange interactions J_i between neighboring Ru ions in the ht-phase strongly differ in the lt-phase along each direction of the $LaRuO_4$ plane, leading

to (almost isolated) Ru-Ru spin singlets. The ht-phase is paramagnetic with AFM exchange of the Ru^{4+} spins ($S = 1$). This behavior is in agreement with the high-temperature limit of the 2D Heisenberg model. The very small magnetic susceptibility in the lt-phase cannot be described by a 2D AFM Heisenberg model. The dimerization transition is of first order, which is clearly observable in the single-crystal susceptibility data and only is smeared out in the polycrystals due to a two-phase coexistence in this temperature range.[22,35] At temperatures below 50 K, the lamellarly arranged twin domains in the single crystals cause a small ferromagnetic contribution to χ due to the interaction of the layers.

The entropy change obtained from the peak in the specific heat at the dimerization transition strongly supports the isolated character of the spin singlets in the lt-phase with only very weak interactions between the dimers. An entropy change of roughly $0.5R\ln(3)$ is found reflecting a significant contribution of the dimer entropy to the total entropy change at T_d, which can be described according to $\Delta S = |R\ln 3 - 0.5S_{\mathrm{dimer}}|$. The singlet state is additionally characterized by a spin-gap, which is large in La_2RuO_5. The values obtained from thermally activated fits of the lt susceptibility just below T_d lead to significantly different results for the polycrystalline sample and the single crystals. Only the former is in agreement with inelastic neutron scattering results, which were also obtained from a polycrystalline sample.[22] The spin-gap as observed in the single crystals is approximately three times larger. The presence of almost isolated spin dimers in a two-dimensional crystal structure is unusual and reveals that even small changes in the interatomic distances can cause the formation of such strongly coupled spin arrangements and have a strong influence on the absolute value of the exchange constants.

ACKNOWLEDGMENTS

The authors gratefully acknowledge Dana Vieweg for the susceptibility measurements and E.-W. Scheidt for providing the fit program for the specific heat. This work was supported by the DFG within the collaborative research unit TRR 80 (Augsburg, Munich).

*stefan.riegg@physik.uni-augsburg.de

[1] M. Hase, I. Terasaki, and K. Uchinokura, Phys. Rev. Lett. **70**, 3651 (1993).
[2] M. Isobe and Y. Ueda, J. Phys. Soc. Jpn. **65**, 1178 (1996).
[3] H. Iwase, M. Isobe, Y. Ueda, and H. Yasuoka, J. Phys. Soc. Jpn. **65**, 2397 (1996).
[4] M. Onoda and N. Nishiguchi, J. Solid State Chem. **127**, 359 (1996).
[5] W. E. Pickett, Phys. Rev. Lett. **79**, 1746 (1997).
[6] M. Matsuda, K. Katsumata, H. Eisaki, N. Motoyama, S. Uchida, S. M. Shapiro, and G. Shirane, Phys. Rev. B **54**, 12199 (1996).
[7] J. Kikuchi, K. Motoya, T. Yamauchi, and Y. Ueda, Phys. Rev. B **60**, 6731 (1999).
[8] A. N. Vasil'ev, M. M. Markina, and E. A. Popova, Low Temp. Phys. **31**, 203 (2005).
[9] T. Yokoo, T. Sakaguchi, K. Kakurai, and J. Akimitsu, J. Phys. Soc. Jpn. **64**, 3651 (1995).
[10] Y. Uchiyama, Y. Sasago, I. Tsukada, K. Uchinokura, A. Zheludev, T. Hayashi, N. Miura, and P. Boni, Phys. Rev. Lett. **83**, 632 (1999).
[11] A. N. Vasiliev, O. L. Ignatchik, M. Isobe, and Y. Ueda, Phys. Rev. B **70**, 132415 (2004)
[12] F. D. M. Haldane, Phys. Lett. A **93**, 464 (1983).
[13] E. Pytte, Phys. Rev. B **10**, 4637 (1974).
[14] L. J. de Jongh, *Magnetic Properties of Layered Transition Metal Compounds* edited by L. J. de Jongh (Kluwer Academic Publishers, Dordrecht, 1990), pp. 1–51.
[15] E. Dagotto and T. M. Rice, Science **271**, 618 (1996).
[16] G. Cao, C. S. Alexander, S. McCall, J. E. Crow, and R. P. Guertin, Mater. Sci. Eng. B **63**, 76 (1999).
[17] R. J. Cava, Dalton Transact. **2004**, 2979 (2004).
[18] R. J. Bouchard and J. F. Weiher, J. Solid State Chem. **4**, 80 (1972).
[19] S. G. Ebbinghaus, E.-W. Scheidt, and T. Götzfried, Phys. Rev. B **75**, 144414 (2007).
[20] C. Dussarrat, F. Grasset, R. Bontchev, and J. Darriet, J. Alloys Compd. **233**, 15 (1996).
[21] S. Ebbinghaus, Z. Hu, and A. Reller, J. Solid State Chem. **156**, 194 (2001).
[22] P. Khalifah, R. Osborn, Q. Huang, H. W. Zandbergen, R. Jin, Y. Liu, D. Mandrus, and R. J. Cava, Science **297**, 2237 (2002).
[23] P. Boullay, D. Mercurio, A. Bencan, A. Meden, G. Drazic, and M. Kosec, J. Solid State Chem. **170**, 294 (2003).
[24] S. G. Ebbinghaus, Acta Crystallogr. Sect. C **61**, i96 (2005).
[25] S. K. Malik, D. C. Kundaliya, and R. D. Kale, Solid State Commun. **135**, 166 (2005).
[26] D. I. Khomskii and T. Mizokawa, Phys. Rev. Lett. **94**, 156402 (2005).
[27] Hua Wu, Z. Hu, T. Burnus, J. D. Denlinger, P. G. Khalifah, D. G. Mandrus, L.-Y. Jang, H. H. Hsieh, A. Tanaka, K. S. Liang, J. W. Allen, R. J. Cava, D. I. Khomskii, and L. H. Tjeng, Phys. Rev. Lett. **96**, 256402 (2006).
[28] S. J. Blundell, T. Lancaster, P. J. Baker, W. Hayes, F. L. Pratt, T. Atake, D. S. Rana, and S. K. Malik, Phys. Rev. B **77**, 094424 (2008).
[29] V. Eyert, S. G. Ebbinghaus, and T. Kopp, Phys. Rev. Lett. **96**, 256401 (2006).
[30] V. Eyert and S. G. Ebbinghaus, Prog. Solid State Chem. **35**, 433 (2007).
[31] K. Motida and S. Miyahara, J. Phys. Soc. Jpn. **28**, 1188 (1970).
[32] M. V. Eremin, Fizika Tverdogo Tela (Physics of the Solid State) **18**, 2088 (1976).
[33] P. W. Anderson, Phys. Rev. **115**, 2 (1959).
[34] D. Zakharov, H.-A. Krug von Nidda, M. Eremin, J. Deisenhofer, R. Eremina, and A. Loidl, *NATO Science for Peace and Security Series B: Physics and Biophysics, Quantum-Magnetism*, edited by B. Barbara *et al.*, pp. 193 (2008).
[35] S. Riegg, U. Sazama, M. Fröba, A. Reller, and S. G. Ebbinghaus, Phys. Rev. B **84**, 014403 (2011).
[36] S. Riegg, A. Reller, and S. G. Ebbinghaus, J. Solid State Chem. **188**, 17 (2012).
[37] G. S. Rushbrooke and P. J. Wood, Mol. Phys. **1**, 257 (1958).

[38]O. Hellwig, T. L. Kirk, J. B. Kortright, A. Berger, and E. E. Fullerton, Nat. Mater. **2**, 112 (2003).
[39]C. Mocuta, A. Barbier, S. Lafaye, P. Bayle-Guillemaud, and M. Panabiere, Phys. Rev. B **68**, 014416 (2003).
[40]C. Leighton, M. R. Fitzsimmons, P. Yashar, A. Hoffmann, J. Nogues, J. Dura, C. F. Majkrzak, and I. K. Schuller, Phys. Rev. Lett. **86**, 4394 (2001).
[41]S.-T. Hong and A. W. Sleight, J. Solid State Chem. **128**, 251 (1997).
[42]J. T. Rijssenbeek, R. Jin, Yu. Zadorozhny, Y. Liu, B. Batlogg, and R. J. Cava, Phys. Rev. B **59**, 4561 (1999).
[43]L. N. Bulaevskii, A. I. Buzdin, and D. I. Khomskii, Solid State Commun. **27**, 5 (1978).
[44]D. Guo, T. Kennedy, and S. Mazumdar, Phys. Rev. B **41**, 9592 (1990).
[45]S. Riegg, A. Günther, H.-A. Krug von Nidda, A. Reller, A. Loidl, and S. G. Ebbinghaus, Eur. Phys. J. B. (unpublished).
[46]T. Hotta and E. Dagotto, Phys. Rev. Lett. **88**, 017201 (2001).